ELSEVIER

Journal of Alloys and Compounds 275–277 (1998) 560–564

Journal of ALLOYS AND COMPOUNDS

Magnetic properties of the high-temperature superconductor $R_2Ba_4Cu_7O_{15-\delta}$ (R=Er, Dy)

G. Böttger[a], P. Allenspach[a,*], J. Mesot[a], A. Dönni[b], Y. Aoki[c], H. Sato[c]

[a]*Laboratory for Neutron Scattering ETHZ and PSI, CH-5232 Villigen PSI, Switzerland*
[b]*Dept. of Physics, Tohoku University, Aoba-ku, Sendai 980-77, Japan*
[c]*Dept. of Physics, Faculty of Science, Tokyo Metropolitan University, Hachioji-shi 192-03, Japan*

Abstract

Specific-heat measurements for $Er_2Ba_4Cu_7O_{15-\delta}$ show a magnetic phase transition at $T_N=0.54$ K for $\delta\approx0.1$ and at $T_N=0.50$ K for $\delta\approx0.7$. While the specific heat data of $Er_2Ba_4Cu_7O_{14.92}$ can be interpreted with an anisotropic 2D-Ising model, the specific heat data of $Er_2Ba_4Cu_7O_{14.30}$ can only be understood by assuming two different types of magnetic clusters to be present in this sample. Such an interpretation is supported by our inelastic neutron data demonstrating the presence of at least two distinctly different surroundings for the rare-earth ions. Furthermore, the importance of dipolar interaction and superexchange for the observed magnetic ordering will be discussed. © 1998 Elsevier Science S.A.

Keywords: Magnetic order; Superexchange; Dipolar interaction; Short-range interaction; Electronic clusters disorder

1. Introduction

A striking feature of the compounds belonging to the $R_2Ba_4Cu_{6+n}O_{14+n-\delta}$ family (R=most rare earth elements; $n=0, 1, 2$; $0\leq\delta\leq1$) is the coexistence of superconductivity and magnetic ordering of the R sublattice at low temperatures. Although the magnetism of two members of this family, namely the $RBa_2Cu_4O_8$ (R-124) and the $RBa_2Cu_3O_{7-\delta}$ (R-123) compounds, has been studied extensively, e.g. [1], [2], little is known about the magnetism in the $R_2Ba_4Cu_7O_{15-\delta}$ (R-247) compounds. Only the magnetic structures of Dy-247 ($\delta\approx0$) with $T_c=60$ K [3] and of Er-247 ($\delta=0.08$) with $T_c=89$ K [4] have been studied.

The compounds of the $R_2Ba_4Cu_{6+n}O_{14+n-\delta}$ family have closely related structures, containing superconducting, buckled CuO_2 planes and linear Cu–O chains. The single Cu–O chains in $RBa_2Cu_3O_{7-\delta}$ ($n=0$) are replaced by double chains in $RBa_2Cu_4O_8$ ($n=2$). The latter is characterised by a fixed oxygen stoichiometry and a fixed T_c of about 80 K. On the other hand the chain structure of 123 displays a variable oxygen stoichiometry ($0\leq\delta\leq1$) and T_c varies from about 94 to 0 K as the oxygen content is decreased. The structure of $R_2Ba_4Cu_7O_{15-\delta}$ ($n=1$) contains alternating 123- and 124-blocks in *c*-direction. While the R^{3+} ions in R-123 are surrounded by two equivalent CuO_2 planes, in R-247 two non-equivalent CuO_2 planes can be found. The single chains can be oxygen depleted as in the R-123 ($n=0$) phase, but the R-247 compound remains superconducting due to the presence of stoichiometric R-124 ($n=2$) blocks. Removing oxygen from the single chains in the 123-blocks lowers T_c from 95 to 30 K [5].

In the $R_2Ba_4Cu_{6+n}O_{14+n-\delta}$ family the R–R distance along the *a*- and *b*-direction is about 3.9 Å, while the distance along the *c*-direction is three times larger. Although the large separation between the R ions along the *c*-axis in R-124 and R-123 should favour two-dimensional (2D) ordering, three-dimensional (3D) ordering has also been reported, e.g. for Er-124 [6] and Er-123 [7]. It is therefore not surprising that Er-247 shows a 3D ordering of the Er ions [4] as well. Since a transition from 3D- to 2D-order of the Er ions can be achieved by oxygen removal in Er-123 [7], we expect a similar behaviour for Er-247 upon oxygen depletion. An investigation of the dependence of the type of magnetic order upon δ in $Er_2Ba_4Cu_7O_{15-\delta}$ is of special interest because Er-247 is expected to be the only compound among the R-247 compounds showing a 3D ordering of the rare-earth ions [3]. Thus, the presumable transition from 3D- to 2D-order in R-247 compounds should be observable in Er-247, only.

*Corresponding author. Tel.: +41 56 310 2527; fax: +41 56 310 2939; e-mail: peter.allenspach@psi.ch

0925-8388/98/$19.00
PII: S0925-8388(98)00391-0

Motivated by this fact, we have performed low temperature heat capacity measurements in order to study the magnetic ordering in $Er_2Ba_4Cu_7O_{15-\delta}$. In this work, we present the results for two $Er_2Ba_4Cu_7O_{15-\delta}$ samples with different oxygen contents δ. As a reference the specific heat and the crystalline electric field (CEF) splitting of $Dy_2Ba_4Cu_7O_{15-\delta}$ (δ=0.05, 0.55) were measured.

2. Experiments

Polycrystalline samples with a nominal composition $R_2Ba_4Cu_7O_{15-\delta}$ with R=Er, Dy were prepared by polymerised complex synthesis [8] starting from R_2O_3, $Ba(NO_3)_2$ and CuO. This method is based on the formation of a polymer–metal complex precursor that is created through polyesterification between metal citrate complexes and ethylene glycol.

We examined the phase purity of our samples by X-ray and neutron powder diffraction, where no impurities could be detected. For the characterisation of superconducting properties, the DC magnetic susceptibility was measured in an applied field of 0.01 T using a Quantum Design SQUID magnetometer. Zero-field cooled susceptibility data have been collected from fine powdered samples, which were fixed with paraffin to prevent reorientation.

The specific heat measurements have been performed in an Oxford ^{3}He–^{4}He dilution cryostat using a semi-adiabatic heat-pulse method. A minimum temperature of 150 mK has been achieved. Samples of about 92 mg were mounted directly into the Cu sample holder in the form of sintered pellets.

The inelastic neutron data have been taken on the triple-axis spectrometer IN3 (Institute Laue Langevin, Grenoble, France) with a Cu monochromator (111) and a pyrolytic graphite analyser (002).

3. Results and discussion

The superconducting transition temperature T_c has been determined by magnetic susceptibility measurements. The $Er_2Ba_4Cu_7O_{15-\delta}$ (δ=0.08) sample shows a T_c=89 K which is close to 95 K, the highest value possible for a fully oxidised 247 sample with δ=0 [5]. The reduced sample $Er_2Ba_4Cu_7O_{15-\delta}$ (δ=0.7) shows a transition to superconductivity at T_c=35 K. The corresponding values for $Dy_2Ba_4Cu_7O_{14.95}$ and $Dy_2Ba_4Cu_7O_{14.45}$ are 91 K and 60 K, respectively.

The specific heat data for the $Er_2Ba_4Cu_7O_{15-\delta}$ samples are displayed in Fig. 1. The Néel temperature T_N has been derived from the peak in the specific heat anomaly, which is associated with the onset of magnetic ordering at 0.54 K for $Er_2Ba_4Cu_7O_{14.92}$ and 0.50 K for $Er_2Ba_4Cu_7O_{14.3}$. Distinct differences can be found between these two Er-247 samples. In $Er_2Ba_4Cu_7O_{14.92}$ a sharp peak is observed, which is typical for long-range magnetic ordering. In $Er_2Ba_4Cu_7O_{14.3}$ on the other hand, this peak shifts slightly to lower temperatures and its height is considerably reduced. In addition, it is superimposed by a broad peak above T_N, which is an indication for either magnetic short-range correlations or a two-level Schottky anomaly [9]. However, a Schottky anomaly can be ruled out, since there is no zero-field splitting of the electronic doublet ground state of Er^{3+} and the first excited doublet lies above 8 meV [10].

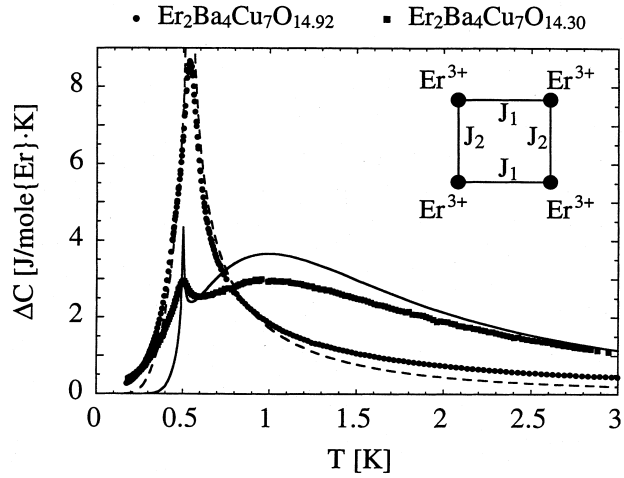

Fig. 1. Magnetic specific heat for $Er_2Ba_4Cu_7O_{14.92}$ and $Er_2Ba_4Cu_7O_{14.3}$. The lines are fits with the anisotropic 2D-Ising model to the data using Onsager's solution [17]. The inset shows the resulting coupling parameters J_1 and J_2 in the (a, b)-plane. The size of these parameters for the two samples are given in Table 1.

For both samples the entropy saturates at the expected value of Rln2 corresponding to the molar entropy of the electronic doublet ground state of Er^{3+}. In $Er_2Ba_4Cu_7O_{14.92}$ about 40% of Rln2 and in $Er_2Ba_4Cu_7O_{14.3}$ about 20% of Rln2 are released at T_N by the magnetic phase transition.

In order to analyze the specific heat data of $Er_2Ba_4Cu_7O_{15-\delta}$ we applied an anisotropic 2D-Ising model [11]. The specific heat of $Er_2Ba_4Cu_7O_{14.92}$ could very well be interpreted by an anisotropic 2D-Ising model (line in Fig. 1). The anisotropy of the magnetic coupling in the plane turns out to be $|J_2/J_1|\approx 1/4$. From the magnetic structure determined by neutron diffraction [4] it is known that the coupling of the Er^{3+} ions along the a-axis is antiferromagnetic (i.e., $J<0$), whereas it is ferromagnetic along the b-axis (i.e., $J>0$), thus we have given the opposite signs to J_1 and J_2 in Table 1. The specific heat data of $Er_2Ba_4Cu_7O_{14.3}$ could not be explained by an anisotropic 2D-Ising model (Fig. 1). This model gives only a qualitative description resulting in an extremely large anisotropy of the coupling parameters. This ratio is 100 times smaller than in $Er_2Ba_4Cu_7O_{14.92}$. As the ratio decreases to values of about 10^{-2} and lower, the behaviour of a 2D-Ising model becomes indistinguishable from that of an isolated Ising chain [9].

Table 1
Coupling constants J_1, J_2 obtained with the anisotropic 2D-Ising model and the cluster model for $Er_2Ba_4Cu_7O_{15-\delta}$ and $Dy_2Ba_4Cu_7O_{15-\delta}$ [a]

	J_1 (meV)	J_2 (meV)
$Er_2Ba_4Cu_7O_{14.92}$		
2D-Ising:	+/−0.039(1)	−/+0.009(1)
$Er_2Ba_4Cu_7O_{14.3}$		
2D-Ising:	+/−0.110(1)	−/+0.0003(10)
20×20 cluster:	+/−0.039	−/+0.009
Chain fragment:	+/−0.120(2)	–
$Dy_2Ba_4Cu_7O_{14.95}$/ $Dy_2Ba_4Cu_7O_{14.45}$		
2D-Ising:	−0.071(1)	−0.017(1)

[a] The signs were taken from the neutron diffraction results [3,4].

This tendency towards one-dimensional behaviour is expected if both dipolar interaction and exchange interaction contribute to the magnetic interaction. MacIsaac et al. [12] obtained a phase diagram of the magnetic ordering in $ErBa_2Cu_3O_{7-\delta}$ by using a Monte-Carlo simulation which includes these two interactions (Fig. 2). Since the spin structure, the lattice constants *a* and *b*, and the magnetic moments of $ErBa_2Cu_3O_{7-\delta}$ and $Er_2Ba_4Cu_7O_{15-\delta}$ are almost identical, this phase diagram should be valid as well for $Er_2Ba_4Cu_7O_{15-\delta}$. For a vanishing or small exchange interaction the magnetic ordering of moments pointing in *b*-direction favours an antiferromagnetic coupling along *a* and a ferromagnetic along *b* (AF/F) as observed in neutron diffraction experiments for both Er-systems [4], [13]. If the exchange interaction is increased, at a certain point the magnetic structure will flip over from AF/F into purely antiferromagnetic (AF/AF). Hence, close to this phase transition from AF/F to AF/AF only one-dimensional antiferromagnetic correlations will persist. In order to understand the specific heat data of $Er_2Ba_4Cu_7O_{15-\delta}$ (and of $ErBa_2Cu_3O_{7-\delta}$) one has to assume an increase of the exchange interaction under oxygen removal. An increase by a factor of three was observed previously for $NdBa_2Cu_3O_{7-\delta}$ by going from $\delta=0$ to $\delta=0.7$ [14]. $NdBa_2Cu_3O_{7-\delta}$ is a system where dipolar interactions are negligible (T_N is to high for dipolar interaction by a factor of 50), therefore the doping dependence of the exchange interaction alone could be investigated. While this phase diagram of MacIsaac et al. can explain the trend towards one-dimensional behaviour (increase of the antiferromagnetic and decrease of the ferromagnetic coupling as a result of the competition between dipolar and exchange interaction) it cannot explain the magnetic structure observed for $Er_2Ba_4Cu_7O_{15-\delta}$ and $ErBa_2Cu_3O_{7-\delta}$ at low oxygen contents which is still AF/F. The onset of the magnetic Cu-ordering may prevent the system from flipping from one to the other configuration.

The magnetic moments in $Dy_2Ba_4Cu_7O_{15-\delta}$ are aligned parallel to the *c*-axis. For such a moment configuration the dipolar interaction favours clearly an AF/AF ordered structure which was observed in neutron diffraction experiments [3]. Hence, an increase of antiferromagnetic exchange within the plane should not affect the magnetic ordering. In Fig. 3, the magnetic specific heat of $Dy_2Ba_4Cu_7O_{14.95}$ and of $Dy_2Ba_4Cu_7O_{14.45}$ are displayed together with an anisotropic 2D-Ising fit (for parameters see Table 1). There is almost no difference between the two data sets besides a small broadening and shrinking of the anomaly for $Dy_2Ba_4Cu_7O_{14.45}$. This broadening originates from the electronic disorder in the CuO_2-planes for intermediate oxygen contents which leads to a disorder in the exchange interaction. While most of the bonds will still be antiferromagnetic some might be ferromagnetic (as observed for $NdBa_2Cu_3O_{7-\delta}$). These ferromagnetic bonds

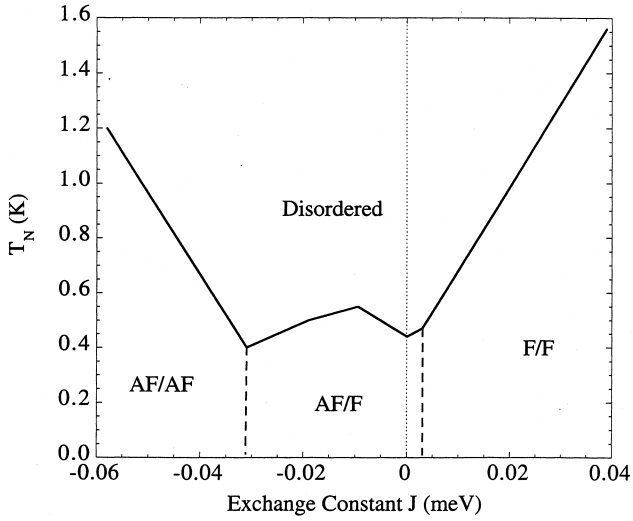

Fig. 2. Phase diagram of Er-123 after MacIsaac et al. [12] (they calculated the phase diagram for Er-123 not for Er-247, but since the moment direction is the same for both systems, it should as well be valid with some scaling for Er-247).

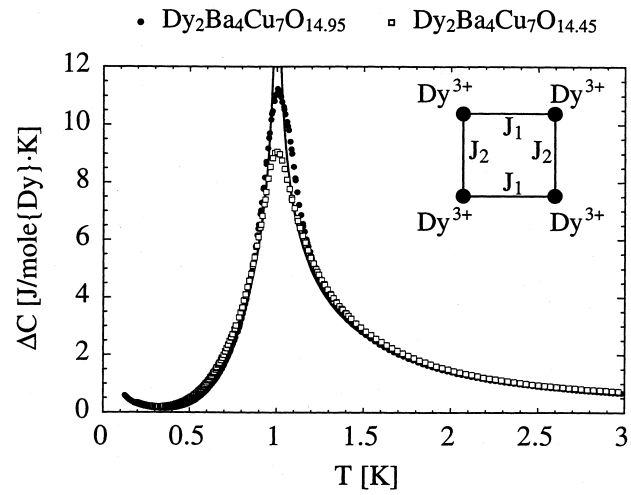

Fig. 3. Magnetic specific heat for $Dy_2Ba_4Cu_7O_{14.95}$ and $Dy_2Ba_4Cu_7O_{14.45}$. The lines are the results of fits with the anisotropic 2D-Ising model. The size of the coupling parameters for the two samples are given in Table 1.

will compete on a local scale with the AF/AF structure preferred by the dipolar interaction and will lead to the observed broadening. For $Er_2Ba_4Cu_7O_{14.3}$ both antiferromagnetic and ferromagnetic exchange interactions depending on the direction may - on a local scale - compete with the dipolar interaction and result in the broad features in the specific heat which will be discussed in the next paragraph.

Since the anisotropic 2D-Ising model cannot explain the specific heat data of $Er_2Ba_4Cu_7O_{14.3}$ quantitatively we introduce a model which treats the sharp peak at T_N and the broader peak above T_N separately. We apply a 2D-Ising cluster model to the sharp peak at T_N which marks an ordered phase similar to the long-range ordered phase in $Er_2Ba_4Cu_7O_{14.92}$. This model is able to reproduce the sharp peak at T_N using a cluster of 20 × 20 Er^{3+} ions and the same coupling parameters as found for $Er_2Ba_4Cu_7O_{14.92}$ ($|J_1|$=0.039 meV and $|J_2|$=0.009 meV; see Table 1 and Fig. 1). For the analysis of the broad peak we assume an isolation of magnetic chains of Er^{3+} ions of finite length for the reasons mentioned above. The only variables are a coupling parameter J describing the coupling in the chain and the chain length. The best result has been achieved by using a chain of 20 ions and a coupling parameter J=0.12 meV (Table 1). Superimposing the results of these fits gives a good agreement with the measured specific heat data (Fig. 4). The volume fractions of the Er^{3+} ions belonging to the clusters and to the chains turn out to be ~25% and ~75%, respectively.

Our heat capacity results show clearly that a reduction of the oxygen content enhances the magnetic anisotropy in Er-247. In addition, the long-range magnetic coupling in the (*a*, *b*)-plane is broken and the system decays into 2D-Ising clusters and 1D-Ising chains according to our analysis.

The existence of superconductivity in 247 even at low oxygen concentrations can be explained in terms of charge redistribution in the CuO_2 planes and between these planes. The situation in $Er_2Ba_4Cu_7O_{14.3}$ can be interpreted in the following way: By removing oxygen from the single chains in the 123-blocks, the amount of holes in the CuO_2 plane is reduced and thereby T_c is lowered. The material becomes more inhomogeneous and superconductivity is realised by a percolation process, which has been shown for Er-123 by inelastic neutron scattering experiments [15]. Recent inelastic neutron scattering experiments of the crystal-field interaction in Er-247 and Dy-247 give some evidence for the same inhomogeneous evolution of superconductivity (Fig. 5 and Ref. [10]). The inhomogeneous properties can be understood as the coexistence of different types of local regions with different hole concentrations. This means for our $Er_2Ba_4Cu_7O_{14.3}$ sample that we have regions with higher and lower hole concentrations. The hole enriched parts in the CuO_2 planes take part in the superconducting process. On the other hand, they support a two-dimensional coupling of the neighbouring Er^{3+} ions via dipolar and nearest-neighbour interaction (mediated by the oxygen atoms in the CuO_2 planes). (That the hole concentration influences the magnetic ordering of the rare earth ions has been shown previously for the R-123 system [14].) Regions of low hole concentration seem to attenuate the magnetic interaction in one direction and enhance it in the other direction, enforcing 1D ordering of the Er^{3+} ions. A similar behaviour has been observed for R-123 systems, e.g. Nd-123 [14] and Er-123 [16]. Hence, there is an almost undisturbed cluster with 2D coupling between the

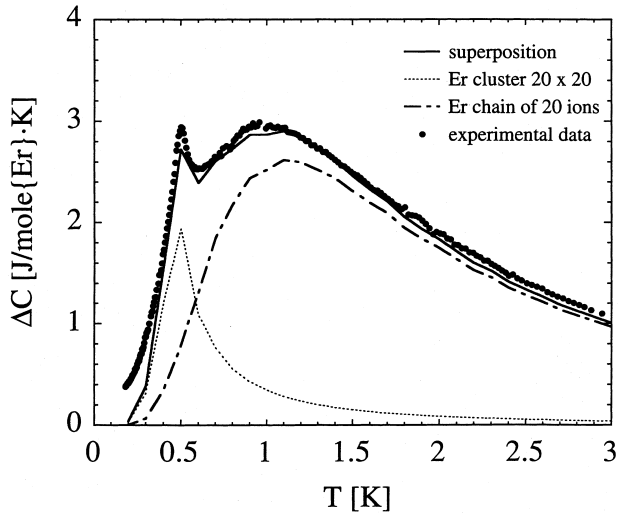

Fig. 4. Magnetic specific heat for $Er_2Ba_4Cu_7O_{14.3}$. The lines are the result of a cluster fit as described in the text.

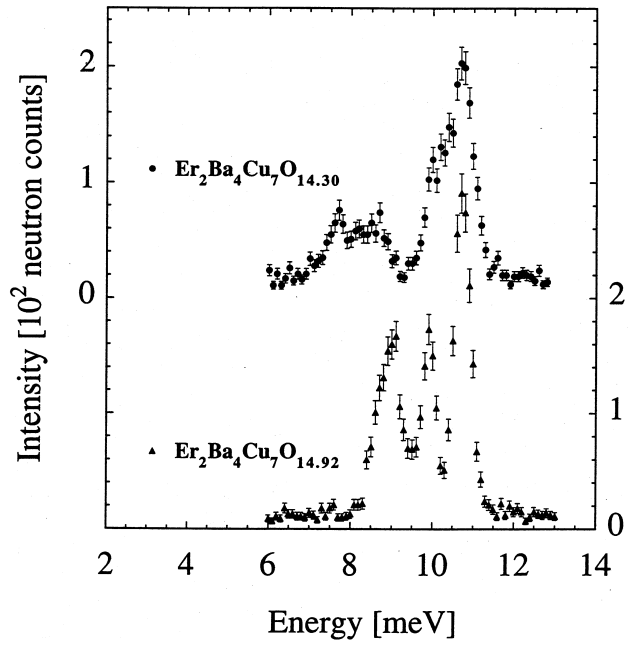

Fig. 5. Neutron spectra of the CEF-splitting of $Er_2Ba_4Cu_7O_{14.92}$ and $Er_2Ba_4Cu_7O_{14.3}$. Instead of three distinct transitions at least four are observed for $Er_2Ba_4Cu_7O_{14.3}$. As for Er-123 this can be attributed to different electronic clusters [15].

Er^{3+} ions as in $Er_2Ba_4Cu_7O_{14.92}$ and electron doped regions with the Er chain fragments. Thus, some Er clusters would be still stable in $Er_2Ba_4Cu_7O_{14.3}$.

4. Conclusion

Distinct differences can be found in the specific heat data of $Er_2Ba_4Cu_7O_{14.92}$ and $Er_2Ba_4Cu_7O_{14.3}$. The specific heat data of $Er_2Ba_4Cu_7O_{14.92}$ are very well described by an anisotropic 2D-Ising model. The anisotropy in the magnetic coupling in the (a, b)-plane is given by $|J_2/J_1| \approx 1/4$. A good description of the specific heat data of $Er_2Ba_4Cu_7O_{14.3}$ has been achieved by using a model consisting of 1D-Ising chains and of 2D-Ising clusters of the Er^{3+} ions. The decay of the magnetic ordering in Er-247 by a reduction of the oxygen content is controlled by the charge redistribution in the CuO_2 planes which results in differently doped regions. However, a reduction of the oxygen content causes a larger magnetic anisotropy and tends to a lowering of the dimensionality and the correlation range of the magnetic interaction of the Er ions. A similar behaviour has been found for the related R-123 compounds [14], [16].

Acknowledgements

The sample preparation by Dr. P. Berastegui is gratefully acknowledged. We thank Dr. K. Conder for the determination of the oxygen content of all samples. This work was supported by the Swiss National Science Foundation and by the Ministry of Education, Science and Culture of Japan.

References

[1] B. Roessli, P. Fischer, U. Staub, M. Zolliker, A. Furrer, Europhys. Lett. 23 (1993) 511.
[2] B. Roessli, P. Fischer, M. Guillaume, J. Mesot, U. Staub, M. Zolliker, A. Furrer, E. Kaldis, J. Karpinski, E. Jilek, J. Phys. Condens. Matter 6 (1994) 4147.
[3] H. Zhang, J.W. Lynn, D.E. Morris, Phys. Rev. B 45 (1992) 10022.
[4] G. Böttger, P. Fischer, A. Dönni, P. Berastegui, Y. Aoki, H. Sato, F. Fauth, Phys. Rev. B 55 (1997) R12005.
[5] J.-Y. Genoud, T. Graf, G. Triscone, A. Junod, J. Muller, Physica C 192 (1992) 137.
[6] H. Zhang, J.W. Lynn, W.-H. Li, T.W. Clinton, D.E. Morris, Phys. Rev. B 41 (1990) 11229.
[7] H. Maletta, E. Pörschke, T. Chattopadhyay, P.J. Brown, Physica C 166 (1990) 9.
[8] P. Berastegui, M. Kakihana, M. Yoshimura, H. Mazaki, H. Yasuoka, L.-G. Johansson, S. Eriksson, L. Börjesson, M. Käll, J. Appl. Phys. 73 (1993) 2424.
[9] R. Navarro, in: L.J. de Jongh (Ed.), Magnetic Properties of Layered Transition Metal Compounds, Kluwer Academic Publishers 1990, pp. 105–190.
[10] G. Böttger, Ph.D Thesis, ETH Zurich, 1998.
[11] G. Böttger, P. Allenspach, A. Dönni, Y. Aoki, H. Sato, Z. Phys. B 104 (1997) 195.
[12] A.B. MacIsaac, J.P. Whitehead, M.C. Robinson, K. De'Bell, Physica B 194–196 (1994) 223.
[13] T. Chattopadhyay, P.J. Brown, D. Bonnenberg, S. Ewert, H. Malleta, Europhys. Lett. 6 (1988) 363.
[14] P. Allenspach, B.W. Lee, D.A. Gajewski, M.B. Maple, G. Nieva, S.-I. Yoo, M.J. Kramer, R.W. McCallum, L. Ben-Dor, Z. Phys. B 96 (1995) 455.
[15] J. Mesot, P. Allenspach, U. Staub, A. Furrer, H. Mutka, Phys. Rev. Lett. 70 (1993) 865.
[16] S. Simizu, G.H. Bellesis, J. Lukin, S.A. Friedberg, H.S. Lessure, S.M. Fine, M. Greenblatt, Phys. Rev. B 39 (1989) 9099.
[17] L. Onsager, Phys. Rev. 65 (1944) 117.